JES
JOURNAL OF ENVIRONMENTAL SCIENCES
ISSN 1001-0742
CN 11-2629/X
February 1, 2014 Volume 26 Number 2
www.jesc.ac.cn

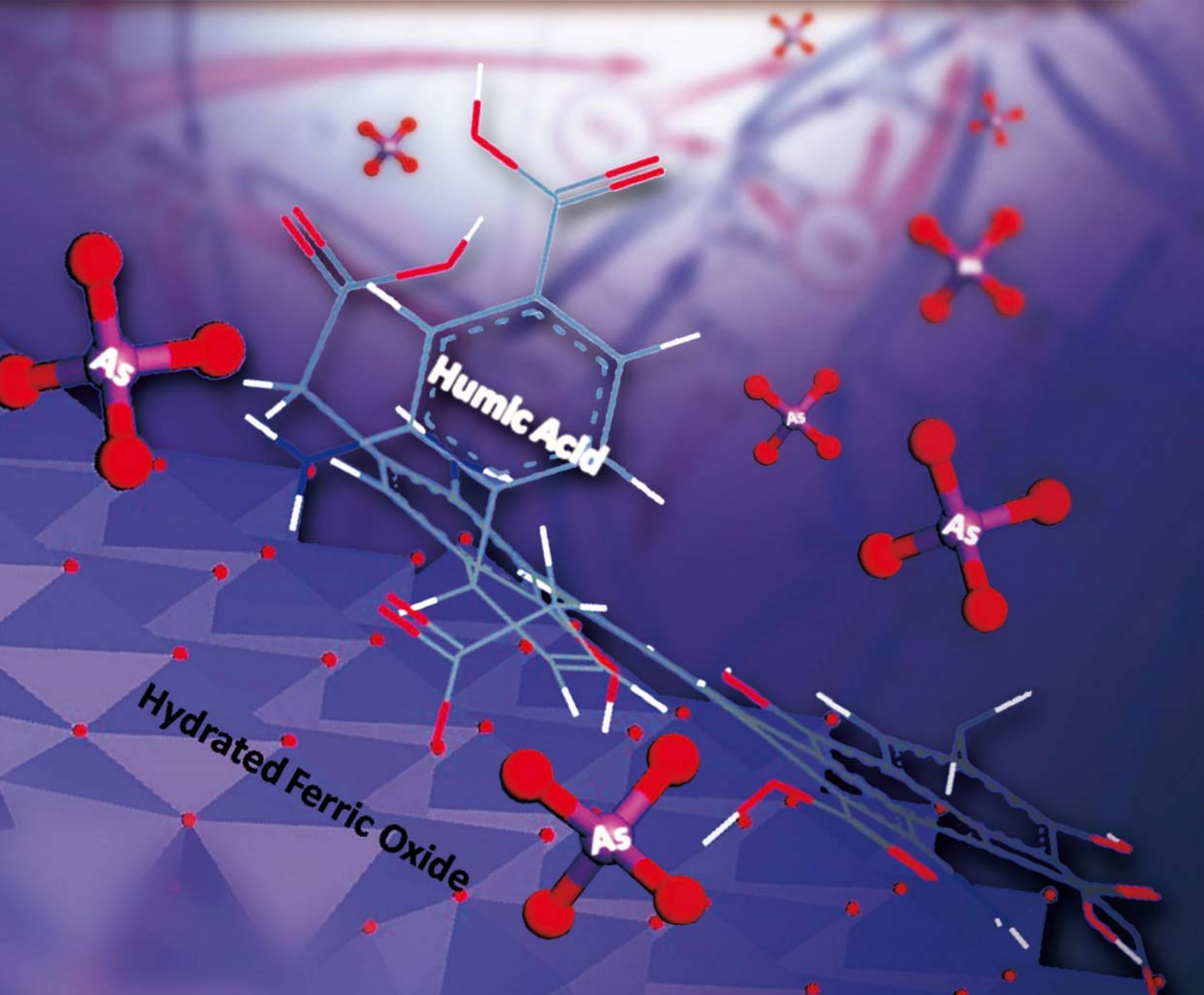

ELSEVIER
Science Press
Sponsored by
Research Center for Eco-Environmental Sciences
Chinese Academy of Sciences

ISSN 1001–0742 **Journal of Environmental Sciences** Vol. 26 No. 2 2014

CONTENTS

Aquatic environment

Atmospheric environment

Environmental health and toxicology

Environmental catalysis and materials

Serial parameter: CN 11-2629/X*1989*m*261*en*P*30*2014-2

Journal of Environmental Sciences 26 (2014) 466–477

Available online at www.sciencedirect.com

Journal of Environmental Sciences

www.jesc.ac.cn

Comparison of quartz sand, anthracite, shale and biological ceramsite for adsorptive removal of phosphorus from aqueous solution

Cheng Jiang[1], Liyue Jia[2], Bo Zhang[1], Yiliang He[1,*], George Kirumba[1]

1. School of Environmental Science and Engineering, Shanghai Jiao Tong University, Shanghai 200240, China. E-mail: jiangcheng2012@aliyun.com
2. School of Urban Construction, Hebei University of Engineering, Handan 056038, China

ARTICLE INFO

Article history:
Received 07 March 2013
revised 06 May 2013
accepted 07 May 2013

Keywords:
quartz sand
anthracite
shale
biological ceramsite
phosphorus
constructed wetlands
DOI: 10.1016/S1001-0742(13)60410-6

ABSTRACT

The choice of substrates with high phosphorus adsorption capacity is vital for sustainable phosphorus removal from waste water in constructed wetlands. In this study, four substrates were used: quartz sand, anthracite, shale and biological ceramsite. These substrate samples were characterized by X-ray diffractometry and scanning electron microscopy studies for their mineral components (chemical components) and surface characteristics. The dynamic experimental results revealed the following ranking order for total phosphorus (TP) removal efficiency: anthracite > biological ceramsite > shale > quartz sand. The adsorptive removal capacities for TP using anthracite, biological ceramsite, shale and quartz sand were 85.87, 81.44, 59.65, and 55.98 mg/kg, respectively. Phosphorus desorption was also studied to analyze the substrates' adsorption efficiency in wastewater treatment as well as the substrates' ability to be reused for treatment. It was noted that the removal performance for the different forms of phosphorus was dependent on the nature of the substrate and the adsorption mechanism. A comparative analysis showed that the removal of particulate phosphorus was much easier using shale. Whereas anthracite had the highest soluble reactive phosphorus (SRP) adsorptive capacity, biological ceramsite had the highest dissolved organic phosphorus (DOP) removal capacity. Phosphorus removal by shale and biological ceramsite was mainly through chemical adsorption, precipitation or biological adsorption. On the other hand, phosphorus removal through physical adsorption (electrostatic attraction or ion exchange) was dominant in anthracite and quartz sand.

Introduction

Constructed wetlands are natural treatment systems that are characterized by the presence of substrate materials and have become a common wastewater treatment option over the last decade (Lazareva and Pichler, 2010). They are regarded as 'environmentally sensitive and cost-effective treatment systems for wastewater renovation' (Hench et al., 2003). They can also be considered as 'ecological engineers' (Tanner, 1996). As an ecological engineering alternative to conventional and chemical methods, the use of constructed wetlands is becoming increasingly popular. Their widespread application is attributed to their low capital investment and excellent pollutant removal efficiencies (Sheng et al., 2012).

Phosphorus is one of the major factors in declining water quality. In this regard, the effective removal of phosphorus from wastewaters has been of growing interest in constructed wetland applications. The wetland ecosystem is composed of the substrate, vegetation and microbial communities. The substrate may play the greatest role and could be the factor most amenable to control (Prochaska and Zouboulis, 2006). Substrates capture high levels of phosphorus and thus aid in realizing low phosphorus concentrations in the effluent. Phosphorus adsorption capacity mainly depends on the type of substrates used in constructed wetlands (Karczmarczyk and Renman, 2011), as well

* Corresponding author. E-mail: ylhe@sjtu.edu.cn

as the substrates' physical-chemical processes (Mateus et al., 2012). Hence, the appropriate choice of substrates is vital in adsorptive removal of phosphorus by means of constructed wetlands (Mateus et al., 2012). It has generally been found that some of these substrates have the potential to enhance the phosphorus removal in constructed wetland systems.

Quartz sand, biological ceramsite and shale are traditional environmental materials that display excellent adsorption properties. Quartz sand is a stable silicate mineral that is widely used as a substrate in water treatment (Xu et al., 2012). In China, biological ceramsite is also widely used as a substrate for constructed wetlands. Shale is also used as a substrate in constructed wetlands. It was reported that shale-based wetlands had 98%–100% phosphorus removal capacity (Mann, 1997). However, their mechanism and performance in phosphorus removal are different. The performance and value of anthracite in its non-fuel uses are not only determined by the well-developed surface area but also the type, number and bonding mode of heteroatoms on the surface (Pietrzak et al., 2007). As a traditional fuel material, anthracite's application as an adsorbent in phosphorus removal is a new research field. Shale and biological ceramsite have higher metal (Ca, Fe, Al or Mg) content as compared to both anthracite and quartz sand. Chemical adsorption, precipitation or biological adsorption mechanisms were therefore responsible for phosphorus removal by shale and biological ceramsite. On the other hand, physical adsorption (electrostatic attraction or ion-exchange) was dominant in anthracite and quartz sand.

This article comparatively analyzes the adsorption capacities of four kinds of substrates. In addition, it explores and explains their different adsorption mechanisms. The practical applicability of the substrates in wastewater was analyzed experimentally under dynamic conditions.

1 Materials and methods

1.1 Materials

The four substrates (quartz sand, anthracite, shale and biological ceramsite) were obtained from Henan Gongyi Hualong Filter Factory, China. The substrates were washed with distilled water to remove the surface-adhered particles. This was to ensure that there were no soluble salts that could be dissolved during the batch studies. The substrates were then dried in an oven at 105°C for 48 hr, to a constant weight. Conversion of the substrates into fine powder was later achieved by grinding with a mechanical grinder. A 20-mesh (850 μm) particle size sieve was used to sieve the samples, which were finally stored in a desiccator for further use.

All reagents were of analytical grade, obtained from Sinopharm Chemical Reagent Co., Ltd. (Shanghai, China). In addition, all solutions were prepared using deionized water. Stock solutions (1000 mg/L) of phosphorus were prepared using anhydrous potassium dihydrogen phosphate (KH_2PO_4) and used throughout the study. The pH was pre-adjusted by HCl and NaOH solutions and measured using a pH meter with a combined pH electrode. The concentrations of phosphorus were determined using the ascorbic acid method with a UNICO spectrophotometer (US-2102 PCS) (Walter, 1961). To analyze the phosphorus removal capacity and practical applicability of the substrates, wastewater was obtained from the Guangdong Heyuan Sewage Treatment Plant effluent. The wastewater's initial Total phosphorus (TP), total dissolved phosphorus (TDP), particulate phosphorus (PP), soluble reactive phosphorus (SRP) and dissolved organic phosphorus (DOP) concentrations were 2.0–2.5 mg/L, 1.5–2.0 mg/L, 0.2–0.5 mg/L, 1.5–2.0 mg/L, and 0.1–0.5 mg/L respectively.

1.2 Phosphorus analysis

Total phosphorus in water can be divided into PP and TDP. TDP can further be divided into inorganic (SRP) and organic (DOP) components (Ellison and Brett, 2006). These forms of phosphorus were determined and analyzed. TP was determined after 30 min of autoclave-mediated digestion (120°C, 100 kPa, with $K_2S_2O_8$ and H_2SO_4) of an unfiltered sample. The molybdenum-blue method was employed for photometric TP analysis. A separate analysis of TDP (a sample of 0.45-μm filtrate was digested and determined as in the TP analysis) was also conducted. The PP was determined by subtracting the TDP from TP (Rinker and Powell, 2006). SRP was also analyzed using the molybdenum-blue method (Murphy and Riley, 1962). The sample was mixed with a reagent containing ammonium molybdate, potassium tartrate and sulphuric acid. Ascorbic acid was then added and a blue complex formed. It was measured using a flow-through detector. For the determination of TDP, organic phosphorus was first oxidized to SRP with the addition of an alkaline potassium persulfate reagent, coupled with heating and UV oxidation. Polyphosphates were oxidized to SRP by sulfuric acid digestion. The sample was then analyzed in a similar manner to SRP. DOP was calculated by subtracting SRP from TDP (Rinker and Powell, 2006). All the above experiments were repeated and the average values used for analysis.

1.3 SEM and XRD analyses

In order to understand more about the surface morphology, microstructures and crystalline phases of the four substrates, the samples were analyzed by scanning electron microscopy (Nova NanoSEM 450, FEI, USA). The SEM images for quartz sand and anthracite (**Fig. 1a** and **b**) revealed the characteristic morphologies of irregular and

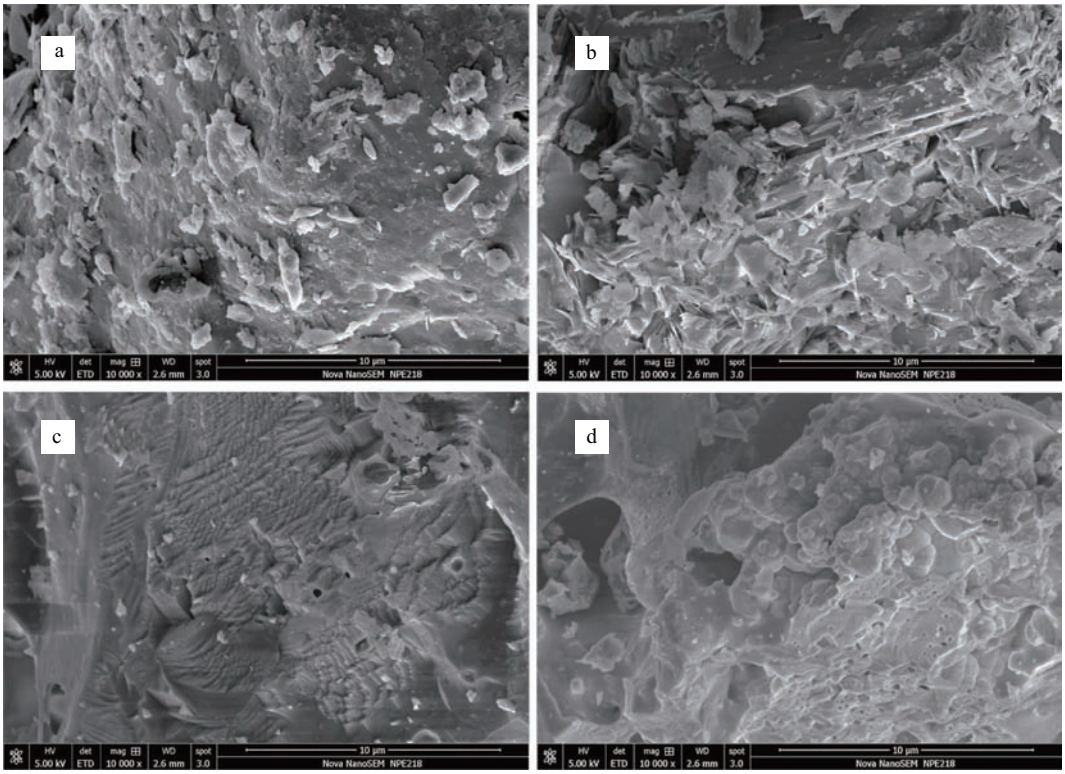

Fig. 1 SEM images for quartz sand (a), anthracite (b), shale (c), biological ceramsite (d).

porous surfaces, indicating high surface areas. On the other hand, the SEM images for shale and biological ceramsite (**Fig. 1c** and **d**) revealed the characteristic morphology of a densified surface and fewer pores. The observed microstructures in the latter samples may be attributed to the high metal content in the substrates.

In this study, mineral compositions (chemical compositions) for the four substrates were determined using X-ray diffraction diffractometer (D8 ADVANCE, Bruker AXS, UK). The samples were scanned for 2θ ranging from 20 to 90°. Identification of the minerals contained in the sample was achieved by comparing the X-ray pattern with a database (Joint Committee on Powder Diffraction Standards-International Centre for Diffraction Data).

Figure 2a reveals quartz crystals (SiO_2) as the predominant mineral of the quartz sand. On the other hand, **Figure 2b** indicates that anthracite was composed of fixed carbon (crystals and amorphous) and amorphous matter. **Figure 2c** indicates that shale was composed of quartz (SiO_2) as well as massive crystals containing Al_2O_3 and Fe_2O_3. **Figure 2d** indicates biological ceramsite was composed of quartz (SiO_2), massive crystals containing Al, Fe and Mg, and other amorphous matter.

The differences in the microstructures and chemical compositions were responsible for the differences in the phosphorus adsorption capacities and mechanisms. The physico-chemical properties of the substrates were the key determinants for phosphorus adsorption.

1.4 Static experiments

The phosphorus static experiments, including the kinetic studies, adsorption isotherms and desorption experiment, were all carried out in batch experiments. A 100-mL conical flasks containing the suspensions were capped and shaken horizontally on a shaker equipped with a thermostat at 120 revolutions per minute (rpm) at 25±1°C. All the above procedures were repeated for several batches and the average values used for analysis.

1.4.1 Adsorption isotherms

Isotherm data were analyzed using Langmuir and Freundlich adsorption equations. The Langmuir and Freundlich parameters were determined and correlation coefficients calculated. The isotherms are used to examine the behavior of different absorbents in attaining adsorption equilibrium (Talip et al., 2009). Adsorption equilibrium is defined as the distribution of the solute between the liquid and the solid phases after the adsorption reaction reaches equilibrium at constant temperature.

The Langmuir isotherm is the theoretical model for monolayer adsorption onto an idealized surface containing a number of identical sites, assuming uniform energy sites on the surface (Tan et al., 2012). The linear forms of the Langmuir isotherms are represented by the following equations (Wahab et al., 2010):

$$\frac{C_e}{Q_e} = \frac{1}{Q_m k_L} + \frac{C_e}{Q_m} \quad (1)$$

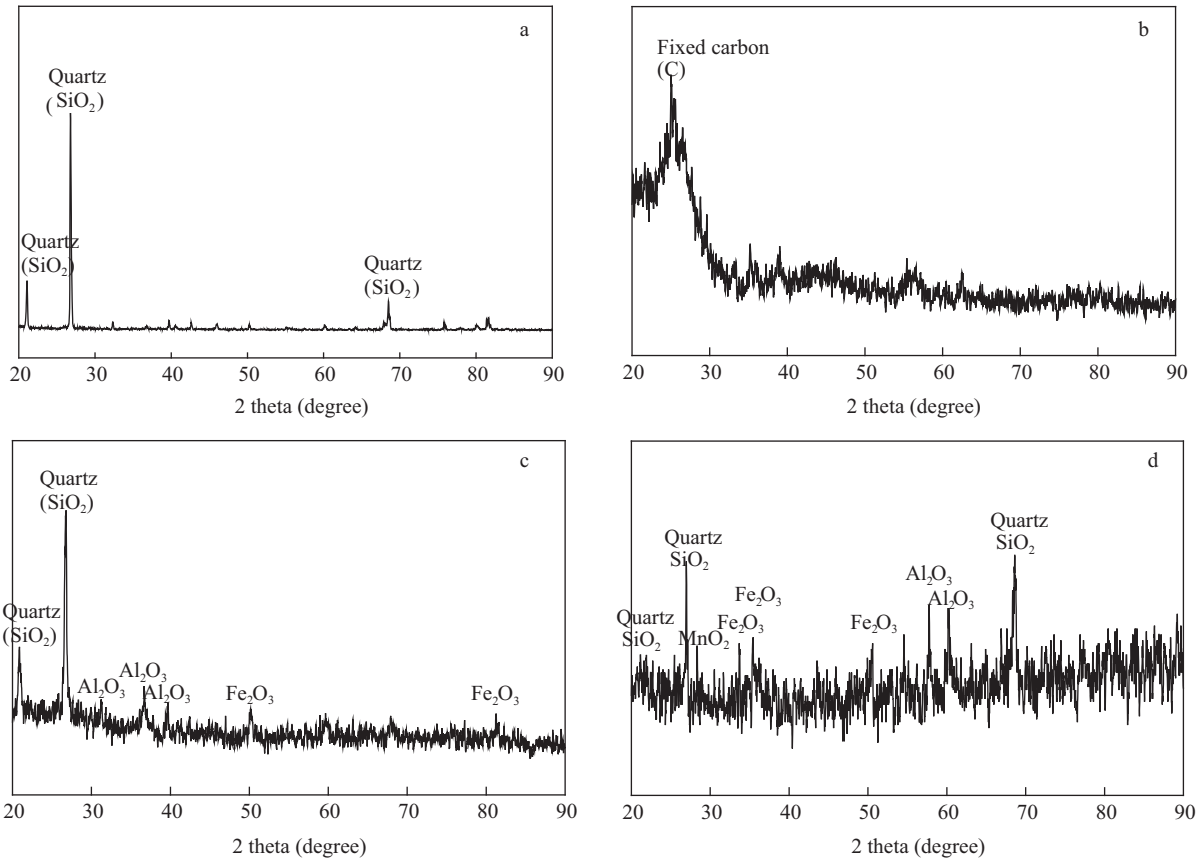

Fig. 2 Powder XRD patterns for quartz sand (a), anthracite (b), shale (c), biological ceramsite (d).

where, Q_e (mg/kg) is the equilibrium phosphorus concentration on the adsorbent, C_e (mg/L) is the equilibrium phosphate concentration in solution, Q_m (mg/kg) is the maximum monolayer phosphorus adsorption capacity of the adsorbent, and k_1 (L/mg) is the binding constant (Fitch, 1990).

The Freundlich isotherm is an empirical equation employed to describe heterogeneous systems (Hameed et al., 2009). The linearized form of the Freundlich isotherm model is written as (Wahab et al., 2010):

$$\log Q_e = \log K_F + \frac{1}{n} \log C_e \quad (2)$$

where, K_F ((mg/kg)/(mg/L)$^{1/n}$) and $1/n$ are the Freundlich constants, which are related to the adsorption capacity and adsorption intensity respectively.

The adsorption isotherm study was carried out by dosing 5 g of the substrates (20-mesh, 850 μm) in 50 mL KH_2PO_4 solutions. Varying phosphorus concentrations ranging from 0 to 40 mg/L were used in solution for 48 hr (i.e. 0, 3, 6, 10, 12, 15, 18, 24, and 40 mg/L). The solution pH was maintained at 7.

1.4.2 Adsorption kinetics

The pseudo second-order kinetic expression for adsorption systems has been applied in a number of studies including those involving the adsorption of anions (Chubar et al., 2005). In this study, the kinetics for the phosphorus ion adsorption was described using a pseudo second-order mechanism. The linearized form of the model is shown below (Wang et al., 2011):

$$\frac{t}{Q_t} = \frac{1}{k_2 Q_e^2} + \frac{t}{Q_e} \quad (3)$$

where, k_2 (kg/(mg·hr)) is the rate constant of the pseudo-second-order kinetic model. The values of equilibrium adsorption capacity (Q_e) and rate constant (k_2) are calculated from the intercept and the slope of the linear plot of t/Q_t versus t, along with the value of the coefficient of determination, R^2.

Adsorption experiments for the kinetic study were carried out by shaking 5 g of the substrates (20-mesh, 850 μm) in 50 mL KH_2PO_4 solutions with an initial concentration of 12 mg/L. The pre-determined contact times for the experiments were 0, 2, 4, 8, 12, 18, 24, 30, and 48 hr. The solution pH was maintained at 7.

1.4.3 Phosphorus desorption

To maximize the removal amount of phosphorus from the wastewater and minimize release of phosphorus retained in the substrate during wastewater treatment, the phosphorus desorption rate was important in the choice of substrates. A low phosphorus desorption rate renders industrial/municipal wastewater treatment more efficient.

After saturation of the substrates (dewatered substrates), the phosphorus desorption analysis was conducted to examine the substrates' behavior in phosphorus release. The efficiency of phosphorus desorption is related to the concentrations of H^+/OH^- (Zhao and Zhao, 2009). Desorption experiments were carried out with pre-sorbed phosphorus-saturated substrates. The phosphorus desorption kinetics were described using a pseudo second-order model. This is described by Eq. (3).

The pH values of the solution were adjusted with HCl or NaOH from 1 to 13. During the phosphorus desorption period, the pH was not controlled. However, it was occasionally monitored and varied slightly during the desorption process. In the analysis, three sets of 1 g phosphorus-saturated substrates were weighed into conical flasks. 50 mL of 0.02 mol/L KCl solution was then added into each conical flask. Three sets of 50 mL 0.02 mol/L KCl solutions without substrates were included as control. The conical flasks were shaken at time intervals of 0.2, 0.5, 1, 1.5, 5, 10, and 20 hr.

1.5 Dynamic experiments

The column experiments were carried out in vertical upflow Plexiglas columns of 595 mm length and 280 mm internal diameter. **Figure 3** shows the general layout of a filled vertical upflow column. All column experiments were run at room temperature (25 ± 1°C). The columns were filled in the following order: A wire screen was placed on the bottom of the column, followed by 200 mm of substrate.

The substrate in the fixed bed column was prewashed by deionized water for several hours. The flow rate at the wastewater inlet was controlled by the metering pump and flowmeter. The wastewater with initial phosphorus concentration of 2.0–2.2 mg/L was allowed to flow into the bottom of the column at a constant rate from the elevated water tank. The effluent was then collected into the water tank. The particle size of the substrates (20-mesh, 850 μm) was consistent with several guidelines for adequate hydraulic conductivity, minimizing the risk of clogging (Vymazal, 2002). This is a consideration factor for long-term application in constructed wetlands systems.

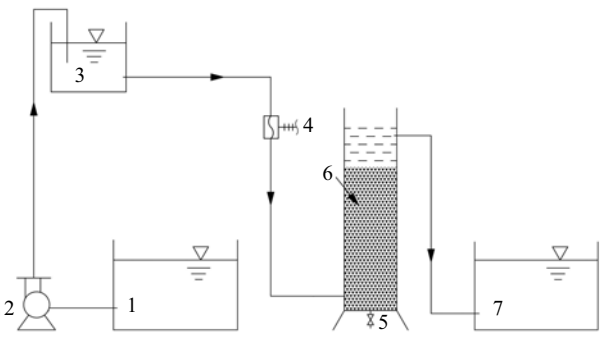

Fig. 3 Schematic diagram of experimental set-up. (1) sewage primary treatment tank; (2) metering pump; (3) elevated water tank; (4) flowmeter; (5) waste recovery outlet; (6) substrate-filled column; (7) effluent tank.

In the first part of the experiments, the design HRT (hydraulic retention time, hr) ranged from 1–8 hr. Based on the experimental result analysis, an optimal HRT of 4 hr was obtained and applied. The HRT was based on measured effluent flow rates using the following Eq. (4) (Tang et al., 2009):

$$\mathrm{HRT} = \frac{\pi r^2 H \varphi}{v} \quad (4)$$

where, r (cm) is the radius of the column, H (cm) is the height of the substrate in the column, φ (%) is the porosity of the substrate and v (mL/hr) is the measured flow rate.

2 Results and discussion

2.1 Adsorption isotherm

The adsorbents/phosphorus isotherms are summarized in **Fig. 4**. It was necessary to describe the goodness of fit for both linear and nonlinear regressions in terms of the correlation coefficient (R^2). **Table 1** shows that the R^2 values of the isotherms were >0.99, indicating that the experimental data fit well to both Langmuir and Freundlich models. Earlier studies involving the analysis of phosphorus adsorption also had similar results (Yan et al., 2010). This suggested that the surfaces of the substrates were made up of small and similar heterogeneous adsorption characteristics (Panuccio et al., 2009). However, it is also very difficult to decide which model represents the experimental data best just on the basis of the regression coefficients (Ayranci and Hoda, 2005).

It was observed that the isotherms were different based on the substrates' adsorption sites and adsorption mechanisms, as indicated by the physical-chemical property analyses (such as SEM and XRD analyses). The Langmuir isotherm is widely used for homogeneous surfaces. The model assumes that the adsorption energy is the same for all surface sites, indicating a monolayer adsorption by the substrates. In this study, as more sites in the substrates were filled up, it became increasingly difficult for a bombarding solute molecule to find an available vacant site. This implies weak competition for active sites. Q_m is the maximum monolayer phosphorus adsorption capacity for the adsorbent, which can generally be used as the theoretical saturated adsorption capacity (Jellali et al., 2011). Comparatively, the Freundlich isotherm is widely employed to describe heterogeneous systems. The model assumes that the frequency of sites associated with free energy of adsorption decreases exponentially with increasing free energy. In addition, the energy of adsorption may vary because real surfaces are heterogeneous surfaces (multilayer adsorption) with a non-uniform distribution (Metaxas et al., 2003). The Freundlich constant K_F value is

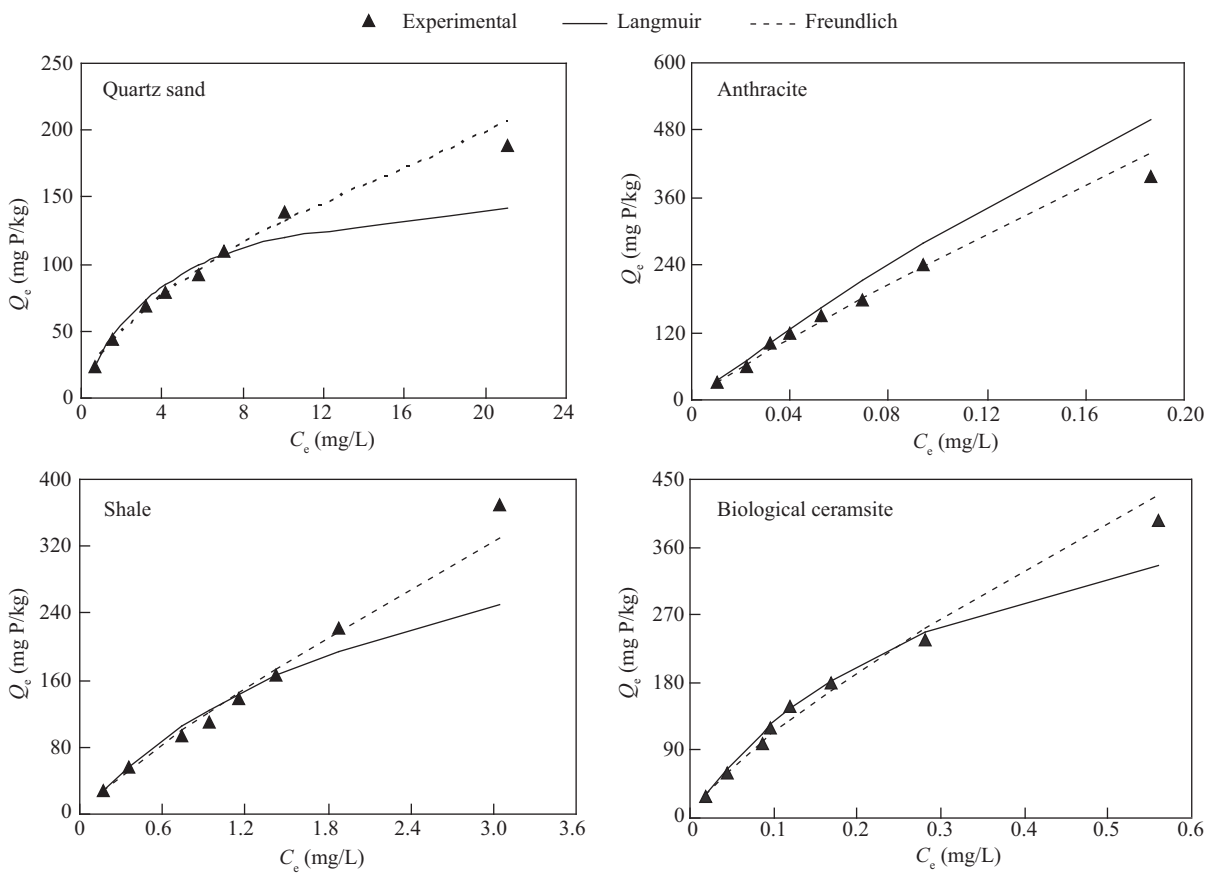

Fig. 4 Phosphorus adsorption isotherm for quartz sand, anthracite, shale, biological ceramsite.

Table 1 Langmuir and Freundlich constants for adsorption of phosphorus by the four substrates

Substrates	Langmuir			Freundlich		
	k_L (L/mg)	Q_m (mg/kg)	R^2	K_F ((mg/kg)/(mg/L)$^{1/n}$)	n	R^2
Quartz sand	0.242	169.49	0.9917	32.696	1.657	0.9930
Anthracite	1.333	2500	0.9967	1976.970	1.115	0.9905
Shale	0.400	454.55	0.9940	127.732	1.173	0.9917
Biological ceramsite	3.167	526.52	0.9975	668.960	1.296	0.9903

also a vital parameter in the determination of a substrate's adsorption behavior and capacity. In summary, **Table 1** shows the following ranking order for phosphorus adsorption capacities: anthracite > biological ceramsite > shale > quartz sand.

Based on these properties, the Freundlich equation is slightly better in describing the adsorption intensity compared to the Langmuir model. In the Freundlich isotherm, the constant *1/n* is a measure of exchange intensity or surface heterogeneity, with values between 0 and 1. In this study, the values of *n* were more than 1 (**Table 1**). This suggested that the adsorption conditions were favorable. High values of *1/n* indicate a strong bond between the substrate and the phosphorus. The obtained *1/n* values for quartz sand, anthracite, shale, and biological ceramsite were 0.6035, 0.8969, 0.8525, and 0.7716, respectively. Based on these values, anthracite had higher adsorption affinity for phosphorus compared to the other substrates.

2.2 Adsorption kinetic modeling

The pseudo-second-order kinetic equation (Eq. (3)) is a reasonably good fit for data over the entire fractional approach to equilibrium. Therefore, it has been employed extensively in the study of adsorption kinetics. As shown in **Table 2**, the correlation coefficients approached unity ($R^2 > 0.99$), implying that the experimental data were reliable. **Figure 5** shows that the adsorption rate (dQ_t/dt) decreases with time until it gradually approaches the equilibrium state. This trend is attributed to the continuous decrease of the driving force ($Q_e - Q_t$).

The adsorption of phosphorus onto the substrates as a function of contact time is shown in **Fig. 5**. The pseudo

second-order model was used to predict the adsorption capacity at equilibrium, Q_e. A comparison showed that the pseudo second-order model values were consistent with the experimental values. This is shown in **Table 2**. In this study, adsorption was a rapid process at the beginning. Results also indicate that all the four substrates attained equilibrium after 8 hr. Many preliminary investigations also revealed that most adsorption of solutes occurred within short contact times. Thereafter, the adsorption rates gradually become slow; hence the adsorption capacity tends to remain constant. In this study, the k_2 values were used to assess the substrates' adsorption characteristics. The values are shown in **Table 2**. For quartz sand, silicon oxide formed complexes in solution. The solid-solution interface of complexes led to development of positive or negative charge on the surface. The charged surface sites on the adsorbent favored the adsorption of phosphate due to electrostatic attraction or ion exchange. Based on its high k_2 value, it was confirmed that anthracite's adsorption capacity was relatively high compared to the other substrates. For anthracite, the structure, with its well-developed surface area and bonding mode of heteroatoms on the surface, fundamentally affects its adsorption behavior. Chemisorption may be due to the fact that the adsorbate species are firmly held onto the adsorbent by comparatively strong bonds. For the shale and biological ceramsite, the reaction products (such as $Fe(OH)_2$ and $Fe(OH)_3$) in water formed a high number of flocs, which could easily fix the phosphorus.

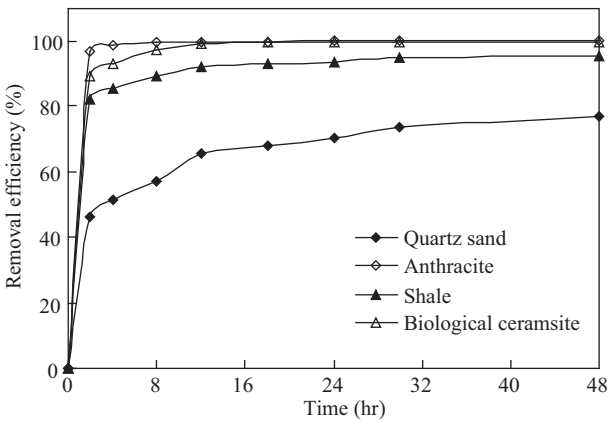

Fig. 5 TP removal efficiency for quartz sand, anthracite, shale and biological ceramsite under different hydraulic retention times.

2.3 Phosphorus desorption study

Table 3 shows that the R^2 values of the desorption kinetics were > 0.99 under different pH conditions. During the desorption experiments, a rapid increase in the substrates' volume was observed when the substrates were placed in water (**Fig. 6**). The initially adsorbed phosphorus diffused back into the water solution. A state of equilibrium was reached after some time. After a desorption period of 20 hr and pH of 7, the phosphorus release contents for quartz sand, anthracite, shale, and biological ceramsite were 12.06, 16.42, 17.85 and 8.57 mg/kg, respectively (**Fig. 6**). However, the equilibrium desorption capacities were calculated using the pseudo second-order model. The corresponding values were 12.15, 16.61, 17.95 and 8.63 mg/kg respectively (**Table 3**). The desorption results suggested that phosphorus was tightly bound to the adsorbents. Based on values presented in **Table 3**, anthracite had the lowest phosphorus desorption rate when pH was 7. It was apparent that the adsorption of phosphorus onto the substrates was the result of chemical bonding and electrostatic attraction. In cases where chemisorption, biological adsorption or ion exchange were involved, poor desorption characteristics were observed. This indicated that these adsorption materials were efficient during wastewater treatment.

The pH seemed to be an important factor affecting the desorption efficiency. The results for phosphorus desorption from phosphorus-saturated substrates by HCl or NaOH at different desorption times are presented in **Fig. 6.** It is clear that most phosphorus was released in the initial stage. The equilibrium was attained within 90 min.

For quartz sand and anthracite, the phosphorus and substrates could form bonds with phosphorus through electrostatic attraction or ion exchange. Therefore, the phosphorus desorption via leaching to the acid or base solution from the phosphorus complex could be expressed by electrostatic sorption energy-loss or charge-transfer. For shale and biological ceramsite, the phosphorus and substrates could form complex compounds through chemical reaction, precipitation or ion exchange. Therefore, the phosphorus desorption via leaching to the acid or base solution from the metal-phosphorus compound could be

Table 2 Kinetics parameters for adsorption of phosphorus by the four substrates

Substrates	$Q_{e,exp}$ (mg/kg)	Pseudo second-order model			
		k_2 (kg/(mg·hr))	Q_e (mg/kg)	R^2	$(Q_e - Q_{e,exp})/Q_e$
Quartz sand	92.32	0.004	96.15	0.9980	0.0399
Anthracite	119.9	0.138	120.48	1.0000	0.0048
Shale	114.33	0.016	114.94	0.9999	0.0054
Biological ceramsite	119.6	0.036	120.48	1.0000	0.0073

$Q_{e,exp}$ was the adsorption content after 48 hr.

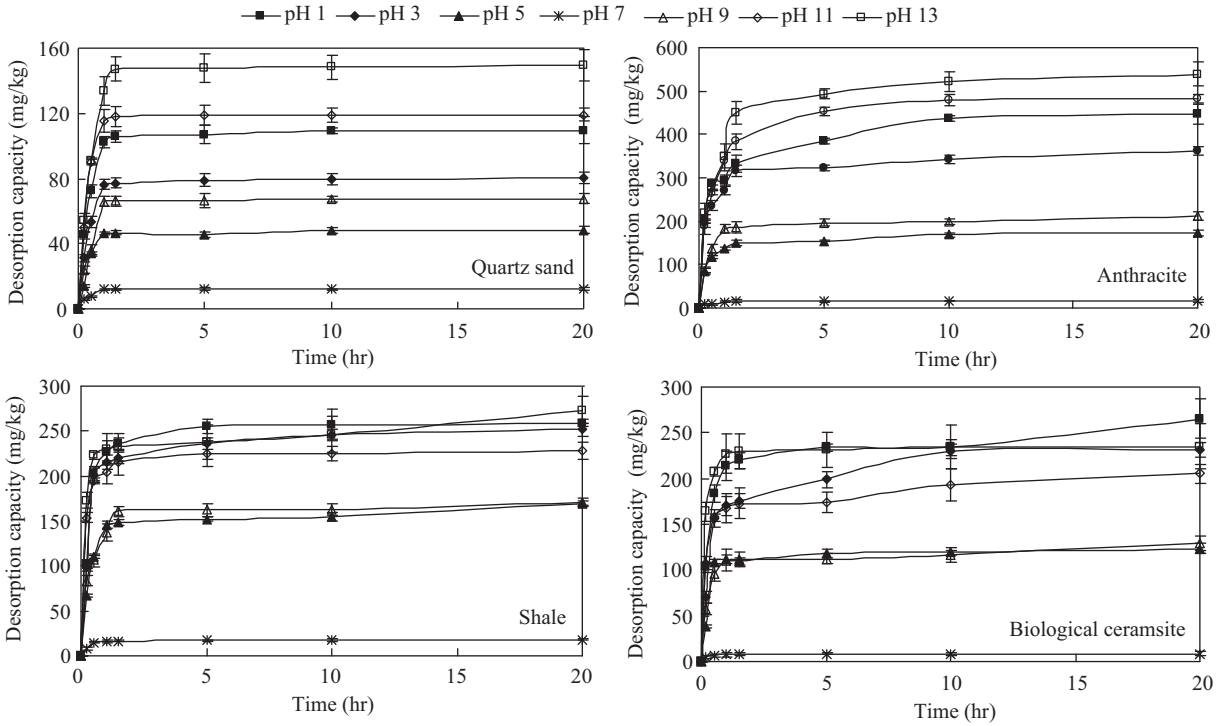

Fig. 6 TP desorption from quartz sand, anthracite, shale, biological ceramsite in different pH solutions under different hydraulic retention times.

Table 3 Equilibrium desorption capacities and desorption rates

Substrates	Pseudo second-ordr model	pH						
		1	3	5	7	9	11	13
Quartz sand	k_2 (kg/(mg·hr))	0.0506	0.0720	0.0894	0.6640	0.0666	0.0689	0.0335
	Q_{ed} (mg/kg)	111.11	81.30	48.78	12.15	68.49	120.48	151.52
	R^2	0.9999	0.9998	0.9995	0.9998	0.9995	0.9998	0.9998
	PPD (%)	65.56	47.97	28.78	7.17	40.41	71.08	89.39
Anthracite	k_2 (kg/(mg·hr))	0.0044	0.0073	0.0171	0.2745	0.0015	0.0050	0.0041
	Q_{ed} (mg/kg)	454.55	370.37	175.44	16.61	212.77	500.00	555.56
	R^2	0.9991	0.9990	0.9994	0.9998	0.9993	0.9999	0.9998
	PPD (%)	18.18	14.81	7.02	0.66	8.51	20.00	22.22
Shale	k_2 (kg/(mg·hr))	0.0206	0.0152	0.0166	0.2927	0.0224	0.0387	0.0114
	Q_{ed} (mg/kg)	263.16	256.41	169.49	17.95	172.41	227.27	270.27
	R^2	0.9999	0.9999	0.9982	0.9999	0.9996	1.0000	0.9969
	PPD (%)	57.89	56.41	37.29	3.95	37.93	49.99	59.46
Biological ceramsite	k_2 (kg/(mg·hr))	0.0090	0.0088	0.0320	0.7033	0.0204	0.0133	0.0588
	Q_{ed} (mg/kg)	263.16	238.10	125.00	8.63	129.87	204.08	238.10
	R^2	0.9964	0.999	0.9996	1.0000	0.9970	0.9981	1.0000
	PPD (%)	49.98	45.22	23.74	1.64	24.67	38.76	45.22

PPD: percent phosphorus desorption; PPD = $\frac{Q_{ed}}{Q_{ts}} \times 100\%$, where, Q_{ts} is theoretical saturated adsorption capacity; Q_{ed} is equilibrium desorption capacity, and it is 169.49, 2500.00, 454.55, and 526.52 mg/kg for quartz sand, anthracite, shale, and biological ceramsite, respectively.

expressed by the chemical equations shown below (M represents a metal ion):

$$MPO_4^{3-} + 3H^+ \rightarrow H_3PO_4 \quad (5)$$

$$MPO_4 + 4OH^- \rightarrow M(OH)_4^- \downarrow + PO_4^{3-} \quad (6)$$

Table 3 shows that the phosphorus desorption rate increased with an increase in acidity/alkalinity. The following ranking order for phosphorus desorption rate was observed: quartz sand > shale > biological ceramsite > anthracite. It was significant to note that the desorption capacity of phosphorus for quartz sand under alkaline conditions was higher compared to that under acidic conditions. For anthracite, the desorption process was dominated by energy loss between the phosphorus and substrate surface. The loss of more electrostatic attraction energy between phosphorus and substrate in the presence of OH^- compared to H^+ was observed. However, for shale and biological ceramsite, the desorption capacities were slightly higher in acidic conditions compared to alkaline conditions.

2.4 Relationship between removal of different phosphorus and HRT

The column batch experiments were more reliable because they had a greater resemblance to the flux conditions in full-scale constructed wetlands than short-term stirred batch experiments (Mateus and Pinho, 2010). The column batch experiments were used to examine the substrates' phosphorus removal under varying HRT. A reasonable HRT not only maximizes the removal of phosphorus but also maintains the stability of the treatment efficiency (Ghosh and Gopal, 2010).

In the study, the phosphorus removal efficiency of each substrate increased with increasing HRT. This is shown in **Fig. 7**. The adsorptive removal of phosphorus stabilized basically after a HRT of 4 hr. The adsorptive removal of various forms phosphorus (TP, TDP, PP, DOP and SRP) was also analyzed. Under a HRT of 4 hr, the TP, TDP and SRP removal efficiencies for anthracite were the highest for all the substrates. Considering the structure of the substrates, anthracite possessed some favorable characteristics, such as higher surface area and higher surface energy. On the other hand, the DOP removal efficiencies for biological ceramsite were the highest of all the substrates, and the removal efficiency of PP for shale was the highest of all the substrates.

Some previous research has confirmed that very long HRT induced physical/chemical clogging in some substrates and reduced their phosphorus removal capacities (Vohla et al., 2011). In addition, the overall performance of some substrates also did not improve with increasing HRT, and the loss of binding capacity was most rapid in the experiment with the longest HRT (Liira et al., 2009). Based on these findings, the optimum HRT for the batch column experiments was 4 hr.

2.5 Various types of phosphorus adsorption from wastewater

In column experiments, several factors such as COD, water turbidity and hydraulic retention time, affect substrates' adsorption of phosphorus from wastewater. The corre-

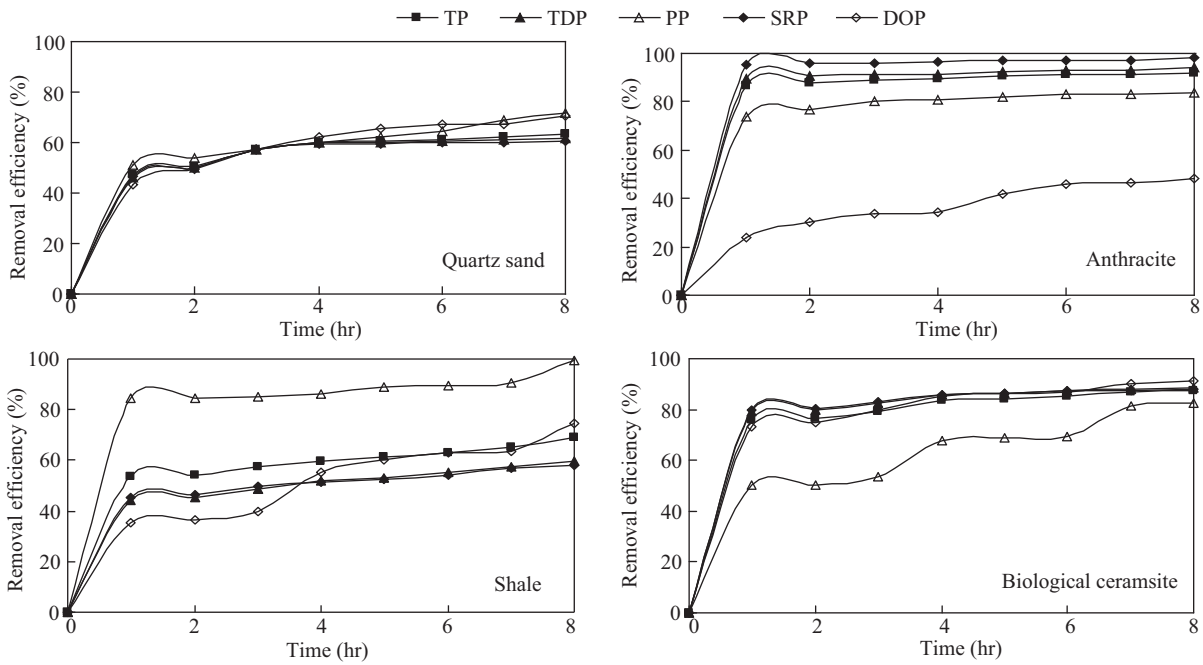

Fig. 7 Adsorptive removal efficiency for various types of phosphorus from wastewater onto quartz sand, anthracite, shale, and biological ceramsite under different HRT.

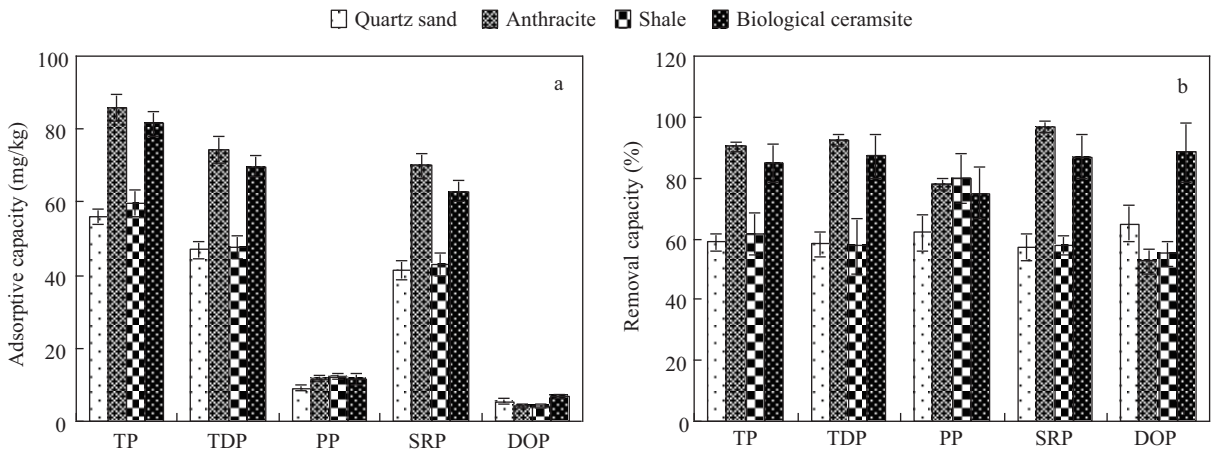

Fig. 8 Adsorptive capacity (a) and adsorptive removal efficiency (b) for various types of phosphorus from wastewater onto quartz sand, anthracite, shale and biological ceramsite.

sponding concentration values for COD_{Cr}, BOD_5, water turbidity and pH for the water samples ranged 45–55, 8–14 and 7.0–8.5 mg/L, respectively. The influence of these parameters on phosphorus adsorption produced better results for static experiments as compared to dynamic experiments. Earlier studies have revealed that adequate concentrations of calcium (Ca), iron (Fe) or aluminum (Al) enhance phosphorus removal efficiencies (Vymazal, 2004). **Figure 8** shows the results of the batch column experiments under a HRT of 4 hr. Whereas the TP removal efficiencies for anthracite, biological ceramsite, shale and quartz sand were 90.35%, 85.03%, 61.34%, 58.81%, respectively, the corresponding adsorptive capacities were 85.87, 81.44, 59.65 and 55.98 mg/kg respectively.

Experimental results revealed that PP could easily be removed by shale. The removal efficiency and capacity were 79.83% and 12.22 mg/kg respectively. Similarly, the removal efficiency and removal capacity of PP using biological ceramsite were 74.98% and 11.65 mg/kg, respectively. The formation of organic/inorganic coprecipitates or the inclusion of PP by metal-phosphorus binding (Ca, Al, Fe, or Mn) into organic aggregates is responsible for the removal of particulate phosphorus. Sorption or coprecipitation processes involving colloidal oxides or oxide-hydroxides are also important.

The removal of TDP by anthracite was much easier compared to the other substrates. Consequently, the highest removal capacity for TDP was observed with anthracite. The TDP removal efficiency and removal capacity were 92.61% and 74.29 mg/kg respectively. SRP removal was superior to DOP removal when anthracite was considered. This implied that a great percentage of the adsorbed TDP was indeed SRP. The latter's removal capacity and removal efficiency were 97.01% and 70.09 mg/kg. The substrate/phosphorus systems had a highly polar solute and substrate, but a non-polar solvent. In the systems, the monofunctional-ion substances with very strong intermolecular attraction were adsorbed from water as a result of ion-ion attraction. It is possible that the adsorbed ions may have become associated into very large clusters just before adsorption took place. This relatively high adsorption capacity shows the strong electrostatic force of attraction between the phosphorus species and the substrates' bonding sites (Kaewsarn and Yu, 2001). In this study, ion-ion attraction or ion exchange was responsible for SRP adsorption by anthracite.

The removal of DOP by biological ceramsite was easier compared to the other substrates. The removal efficiency and removal capacity of DOP was 88.28% and 6.81 mg/kg respectively. The biological ceramsite was dependent on the suspended microbes and attached microbes for biological DOP removal. The lowest phosphorus removal capacity was observed when quartz sand was considered. This is attributed to the electrostatic attraction employed by the substrate in the adsorption mechanism.

3 Conclusions

This study focused on the mechanism and adsorption capability of wetland substrates (quartz sand, anthracite, shale and biological ceramsite) during phosphorus removal processes. In treating wastewater using shale and biological ceramsite, chemical adsorption, precipitation or biological adsorption occurred. On the other hand, when treating wastewater using quartz sand and anthracite, the strong electrostatic force of attraction between phosphorus and the substrates was due to ion-ion attraction or ion exchange. The different adsorption mechanisms and significantly higher adsorption capacities for quartz sand, anthracite, shale and biological ceramsite could be applied to separate different forms of phosphorus in wastewater. Consequently, a choice of which substrate to use for dif-

ferent kinds of wastewater can be made. Further practical application of these substrates in constructed wetland treatment systems should be enhanced for future sustainability in industrial/municipal wastewater treatment.

In addition, the study also analyzed phosphorus desorption. In neutral solution, the substrates had low desorption rates, indicating that these adsorption materials were efficient during wastewater treatment. However, the phosphorus desorption rate was clearly higher under acidic/alkaline conditions as compared to neutral conditions.

Acknowledgment

This work was supported by the Important National Science and Technology Specific Projects (No. 2013ZX07206001), the National Research Foundation Singapore under its Campus for Research Excellence and Technological Enterprise, and Science and Technology Commission of Shanghai Municipality Projects (No. 09DZ1200109). The authors thank fellow colleagues for their help and valuable advice. The authors also express their sincere gratitude to all the editors and reviewers of this manuscript.

REFERENCES

Ayranci, E., Hoda, N., 2005. Adsorption kinetics and isotherms of pesticides onto activated carbon-cloth. Chemosphere 60, 1600–1607.

Chubar, N. I., Kanibolotskyy, V. A., Strelko, V. V., Gallios, G. G., Samanidou, V. F., Shaposhnikova, T. O. et al., 2005. Adsorption of phosphate ions on novel inorganic ion exchangers. Colloids Sur. A 255, 55–63.

Ellison, M. E., Brett, M. T., 2006. Particulate phosphorus bioavailability as a function of stream flow and land cover. Water Res. 40, 1258–1268.

Fitch, B., 1990. Solid-liquid Separation. Edited by Ladislav Svarovski, third ed. Butterworths, Stoneham. 1780–1781.

Ghosh, D., Gopal, B., 2010. Effect of hydraulic retention time on the treatment of secondary effluent in a subsurface flow constructed wetland. Ecol. Eng. 36, 1044–1051.

Hameed, B. H., Salman, J. M., Ahmad, A. L., 2009. Adsorption isotherm and kinetic modeling of 2, 4-D pesticide on activated carbon derived from date stones. J. Hazard. Mater. 163, 121–126.

Hench, K. R., Bissonnette, G. K., Sexstone, A. J., Coleman, J. G., Garbutt, K., Skousen, J. G., 2003. Fate of physical, chemical, and microbial contaminants in domestic wastewater following treatment by small constructed wetlands. Water Res. 37, 921–927.

Kaewsarn, P., Yu, Q., 2001. Cadmium(II) removal from aqueous solutions by pre-treated biomass of marine alga *Padina* sp. Environ. Pollut. 112, 209–213.

Karczmarczyk, A., Renman, G., 2011. Phosphorus Accumulation pattern in a subsurface constructed wetland treating residential wastewater. Water 3, 146–156.

Lazareva, O., Pichler, T., 2010. Long-term performance of a constructed wetland/filter basin system treating wastewater, Central Florida. Chem. Geol. 269, 137–152.

Liira, M., Kõiv, M., Mander, Ü., Mõtlep, R., Vohla, C., Kirsimäe, K., 2009. Active filtration of phosphorus on Ca-rich hydrated oil-shale ash: does longer retention time improve the process? Environ. Sci. Techn. 43, 3809–3814.

Jellali, S., Wahab, M. A., Hassine, R. B., Hamzaoui, A. H., Bousselmi, L., 2011. Adsorption characteristics of phosphorus from aqueous solutions onto phosphate mine wastes. Chem. Eng. J. 169, 157–165.

Mann, R. A., 1997. Phosphorus adsorption and desorption characteristics of constructed wetland gravels and steelworks by-products. Soil Res. 35, 375–384.

Mateus, D. M. R., Pinho, H. J. O., 2010. Phosphorus removal by expanded clay six years of pilot-scale constructed wetlands experience. Water Environ. Res. 82, 128–137.

Mateus, D. M. R., Vaz, M. M. N., Pinho, H. J. O., 2012. Fragmented limestone wastes as a constructed wetland substrate for phosphorus removal. Ecol. Eng. 41, 65–69.

Metaxas, M., Kasselouri-Rigopoulou, V., Galiatsatou, P., Konstantopoulou, C., Oikonomou, D., 2003. Thorium removal by different adsorbents. J. Hazard. Mater. 97, 71–82.

Murphy, J., Riley, J. P., 1962. A modified single solution method for the determination of phosphate in natural waters. Anal. Chim. Acta 27, 31–36.

Panuccio, M. R., Sorgon, A., Rizzo, M., Cacco, G., 2009. Cadmium adsorption on vermiculite, zeolite and pumice: Batch experimental studies. J. Environ. Manag. 90, 363–374.

Pietrzak, R., Jurewicz, K., Nowicki, P., Babeł, K., Wachowska, H., 2007. Microporous activated carbons from ammoxidised anthracite and their capacitance behaviours. Fuel 86, 1086–1092.

Prochaska, C. A., Zouboulis, A. I., 2006. Removal of phosphates by pilot vertical-flow constructed wetlands using a mixture of sand and dolomite as substrate. Ecol. Eng. 26, 293–303.

Rinker, K. R., Powell, R. T., 2006. Dissolved organic phosphorus in the Mississippi River plume during spring and fall 2002. Mar. Chem. 102, 170–179.

Sheng, S., Rui, J. L., Chen, Y. C., Wang, Y. L., Tao, R. J., Wei, J., 2012. Different constructed wetland substrates and their applications. Adv. Mater. Res. 399-401, 1222–1225.

Talip, Z., Eral, M., Hiçsönmez, Ü., 2009. Adsorption of thorium from aqueous solutions by perlite. J. Environ. Radioact. 100, 139–143.

Tan, J. W., Su, W., Dou, T. J., Fan, X. P., 2012. Adsorption of Ce(IV) ions from aqueous solution by silica aerogels. Separat. Sci. Technol. 47, 1149–1155.

Tang, X. Q., Huang, S. L., Scholz, M., 2009. Comparison of phosphorus removal between vertical subsurface flow constructed wetlands with different substrates. Water Environ. J. 23, 180–188.

Tanner, C. C., 1996. Plants for constructed wetland treatment systems-A comparison of the growth and nutrient uptake of eight emergent species. Ecol. Eng. 7, 59–83.

Vohla, C., Köiv, M., Bavor, H. J., Chazarenc, F., Mander, Ü., 2011. Filter materials for phosphorus removal from wastewater in treatment wetlands–A review. Ecol. Eng. 37, 70–89.

Vymazal, J., 2002. The use of sub-surface constructed wetlands for wastewater treatment in the Czech Republic: 10 years experience. Ecol. Eng. 18, 633–646.

Vymazal, J., 2004. Removal of phosphorus in constructed wetlands with

horizontal sub-surface flow in the Czech Republic. Water, Air, Soil Pollut. 4, 657–670.

Wahab, M. A., Jellali, S., Jedidi, N., 2010. Ammonium biosorption onto sawdust: FTIR analysis, kinetics and adsorption isotherms modeling. Bioresour. Technol. 101, 5070–5075.

Walter, W. G., 1961. Standard methods for the examination of water and wastewater. Amer. J. Public Health Nat. Health 51, 940–940.

Wang, J., Zheng, C., Ding, S., Ma, H., Ji, Y., 2011. Behaviors and mechanisms of tannic acid adsorption on an amino-functionalized magnetic nanoadsorbent. Desalination 273, 285–291.

Xu, C., Shi, J., Zhou, W., Gao, B., Yue, Q., Wang, X., 2012. Bromate removal from aqueous solutions by nano crystalline akaganeite (β-FeOOH)-coated quartz sand (CACQS). Chem. Eng. J. 187, 63–68.

Yan, L. G., Xu, Y. Y., Yu, H. Q., Xin, X. D., Wei, Q., Du, B., 2010. Adsorption of phosphate from aqueous solution by hydroxy-aluminum, hydroxy-iron and hydroxy-iron–aluminum pillared bentonites. J. Hazard. Mater. 179, 244–250.

Zhao, X. H., Zhao, Y. Q., 2009. Investigation of phosphorus desorption from P-saturated alum sludge used as a substrate in constructed wetland. Sep. Purif. Technol. 66, 71–75.

Editorial Board of Journal of Environmental Sciences

JOURNAL OF ENVIRONMENTAL SCIENCES

环境科学学报(英文版)

(http://www.jesc.ac.cn)

Aims and scope

Journal of Environmental Sciences is an international academic journal supervised by Research Center for Eco-Environmental Sciences, Chinese Academy of Sciences. The journal publishes original, peer-reviewed innovative research and valuable findings in environmental sciences. The types of articles published are research article, critical review, rapid communications, and special issues.

The scope of the journal embraces the treatment processes for natural groundwater, municipal, agricultural and industrial water and wastewaters; physical and chemical methods for limitation of pollutants emission into the atmospheric environment; chemical and biological and phytoremediation of contaminated soil; fate and transport of pollutants in environments; toxicological effects of terrorist chemical release on the natural environment and human health; development of environmental catalysts and materials.

For subscription to electronic edition

Elsevier is responsible for subscription of the journal. Please subscribe to the journal via http://www.elsevier.com/locate/jes.

For subscription to print edition

China: Please contact the customer service, Science Press, 16 Donghuangchenggen North Street, Beijing 100717, China. Tel: +86-10-64017032; E-mail: journal@mail.sciencep.com, or the local post office throughout China (domestic postcode: 2-580).

Outside China: Please order the journal from the Elsevier Customer Service Department at the Regional Sales Office nearest you.

Submission declaration

Submission of an article implies that the work described has not been published previously (except in the form of an abstract or as part of a published lecture or academic thesis), that it is not under consideration for publication elsewhere. The submission should be approved by all authors and tacitly or explicitly by the responsible authorities where the work was carried out. If the manuscript accepted, it will not be published elsewhere in the same form, in English or in any other language, including electronically without the written consent of the copyright-holder.

Submission declaration

Submission of the work described has not been published previously (except in the form of an abstract or as part of a published lecture or academic thesis), that it is not under consideration for publication elsewhere. The publication should be approved by all authors and tacitly or explicitly by the responsible authorities where the work was carried out. If the manuscript accepted, it will not be published elsewhere in the same form, in English or in any other language, including electronically without the written consent of the copyright-holder.

Editorial

Authors should submit manuscript online at http://www.jesc.ac.cn. In case of queries, please contact editorial office, Tel: +86-10-62920553, E-mail: jesc@263.net, jesc@rcees.ac.cn. Instruction to authors is available at http://www.jesc.ac.cn.

Journal of Environmental Sciences (Established in 1989)

Vol. 26 No. 2 2014

Supervised by	Chinese Academy of Sciences	**Published by**	Science Press, Beijing, China
Sponsored by	Research Center for Eco-Environmental		Elsevier Limited, The Netherlands
	Sciences, Chinese Academy of Sciences	**Distributed by**	
Edited by	Editorial Office of Journal of	Domestic	Science Press, 16 Donghuangchenggen
	Environmental Sciences		North Street, Beijing 100717, China
	P. O. Box 2871, Beijing 100085, China		Local Post Offices through China
	Tel: 86-10-62920553; http://www.jesc.ac.cn	Foreign	Elsevier Limited
	E-mail: jesc@263.net, jesc@rcees.ac.cn		http://www.elsevier.com/locate/jes
Editor-in-chief	Hongxiao Tang	**Printed by**	Beijing Beilin Printing House, 100083, China

CN 11-2629/X **Domestic postcode: 2-580** **Domestic price per issue RMB ¥ 110.00**

ISSN 1001-0742